Hindawi
Advances in Condensed Matter Physics
Volume 2018, Article ID 7578050, 5 pages
https://doi.org/10.1155/2018/7578050

Research Article

PMMA Sandwiched Bi_2Te_3 Layer as a Saturable Absorber in Mode-Locked Fiber Laser

Guobao Jiang ,[1,2] Yuan Zhou ,[1] Lulu Wang ,[1] and Ying Chen [1,2]

[1] *School of Electronic Information and Electrical Engineering, Changsha University, Changsha 410003, China*
[2] *Key Laboratory for Micro-/Nano-Optoelectronic Devices of Ministry of Education, School of Physics and Electronics, Hunan University, Changsha 410082, China*

Correspondence should be addressed to Ying Chen; yingchen@ccsu.edu.cn

Received 21 June 2018; Accepted 6 December 2018; Published 18 December 2018

Guest Editor: Xinxing Zhou

In this paper, we fabricated a PMMA sandwiched Bi_2Te_3 self-assembly layer as a saturable absorber device, which was used as a passive mode locker for ultrafast pulse generation at the telecommunication band. Nanosheets of Bi_2Te_3 as a bulk topological insulator were successfully synthesized through a solvothermal treatment and self-assemble method to form a thin film at a water-air interface. In order to transfer the Bi_2Te_3 self-assembly layer to the optical fiber end, we design a construction of two PMMA layers sandwiched self-assembly layer. By incorporating this saturable absorber into an erbium-doped fiber laser, femtosecond mode-locking operation was experimentally demonstrated. The output pulse width is about 505 fs. Our results indicate that PMMA sandwiched topological insulator layer structure could be an improvement technology in traditional PMMA transfer method and could be used as a long-term stable saturable absorber for the passively mode locking lasers.

1. Introduction

Topological insulator is a state of quantum matter with insulating bulk states like an ordinary insulator and highly conducting and massless spin-helical surface states on its surface [1–7]. These unique properties, which are derived from the combination of spin-orbit interactions and time-reversal symmetry, enable topological insulators as efficient saturable absorber materials for the generation of ultrafast pulse [8, 9]. Compared with traditional saturable absorbers, such as semiconductor saturable absorber mirrors (SESAMs) [10, 11], single-walled carbon nanotubes (SWCNTs) [12], graphene [13], transitional metal dichalcogenides [14, 15], black phosphorus [16, 17], topological insulator saturable absorber possesses many good qualities, such as low saturable absorption threshold, large modulation depth [18, 19], short recovery time [20, 21], and wavelength independent saturable absorption [22]. To fabricate saturable absorbers with advanced performance, it is necessary to search for a facile and simple transfer technique of topological insulator nanosheets onto target substrates like optical fiber-ferrules or optical quartz substrate.

Several methods have been proposed for the transfer of saturable absorbers onto the optical fiber-ferrules, such as optical deposition [23], ink jet print [24], drop cast [25], and polymer composite [26]. Drop cast is favored for its simple and facility. However, its coffee ring effect is difficult to effectively restrain while drying the solute. Ink jet print method is tedious and prone to error and requires for precision instruments and skillful professional operators. Optical deposition was used to deposit carbon nanotubes and graphene onto cores of optical fiber ends. Though the method is simple, it requires precise control of the optical power and does not possess controllability of the deposition layer properties.

In this paper, we present a simple approach to improve the Bi_2Te_3 (one kind of topological insulator) transfer method. The Bi_2Te_3 nanosheets were deposited on the PMMA film, and then another PMMA film was placed onto the Bi_2Te_3 nanosheets to isolate air and water. By this process, the stability of Bi_2Te_3 based saturable absorber was greatly increased. The sandwiched structure of Bi_2Te_3 film was placed onto fiber end facet and introduced into fiber ring laser. Ultrafast pulse was obtained with sandwiched structure of Bi_2Te_3 film

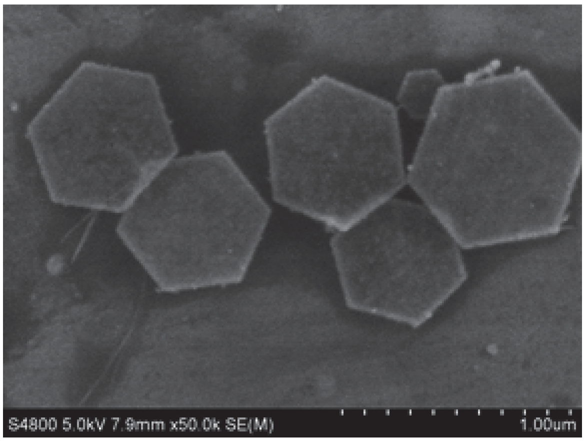

Figure 1: SEM image of Bi_2Te_3 nanosheets.

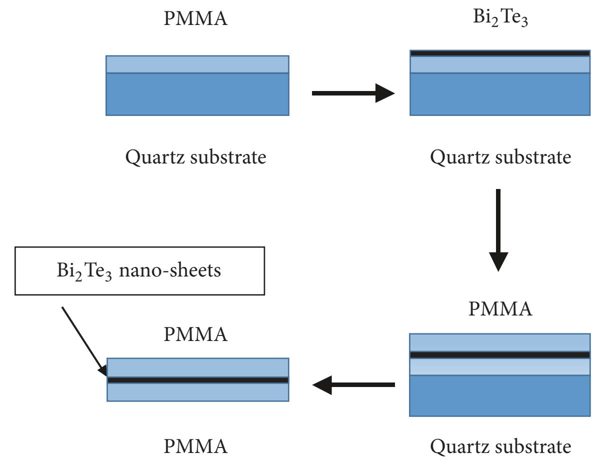

Figure 2: Fabrication of PMMA sandwiched Bi_2Te_3 nanosheets saturable absorber.

saturable absorber. It has a pulse width of about 505 fs and a repetition rate of 13.14 MHz. The stable mode-locking operation lasted at least 6 hours. All these results show that this PMMA sandwiched Bi_2Te_3 structure is an effective and stable saturable absorber, which could have potential applications in ultrafast pulse generation.

2. Saturable Absorber Preparation

2.1. Synthesis of Bi_2Te_3 Nanosheets. Bi_2Te_3 nanosheets were synthesized following a solvothermal method of Wang et al. [27]. Using a typical synthesis, a stoichiometric ratio of bismuth chloride ($BiCl_3$) and sodium selenide (Na_2TeO_3) was dissolved in ethylene glycol with vigorous stirring. Then the mixture was transferred into the Teflon-lined stainless-steel autoclave and heated to 200°C. The autoclave was maintained at the reaction temperature for 36 h and then cooled to room temperature naturally. The black powders were collected by filtering, washed with distilled water and ethanol, and finally dried at 60°C in vacuum overnight. The as-grown and washed powders were dispersed in ethanol solution.

2.2. Characterization of Bi_2Te_3 Nanosheets. Scanning electronic microscope (SEM) measurements were carried out to characterize the morphology of Bi_2Te_3 nanosheets. The SEM image shows that the Bi_2Te_3 sample has a uniform size and shape in Figure 1. The obtained products are predominantly hexagonal-based plates, which matches well with the regular hexagonal lattice structure of Bi_2Te_3.

2.3. Fabrication of Bi_2Te_3 Based Saturable Absorber. Figure 2 shows the fabrication of Bi_2Te_3 based saturable absorber. The PMMA solution was spin coated onto quartz substrate and then the Bi_2Te_3 dispersion was also spin coated onto the PMMA film. Thus the Bi_2Te_3 based saturable absorber was fabricated. To enhance the mechanical strength and stability of the saturable absorber, another PMMA film was placed onto the Bi_2Te_3 nanosheets to isolate air and water. The sandwiched structure was peeled down from the quartz substrate. The Bi_2Te_3 based saturable absorber was completely made.

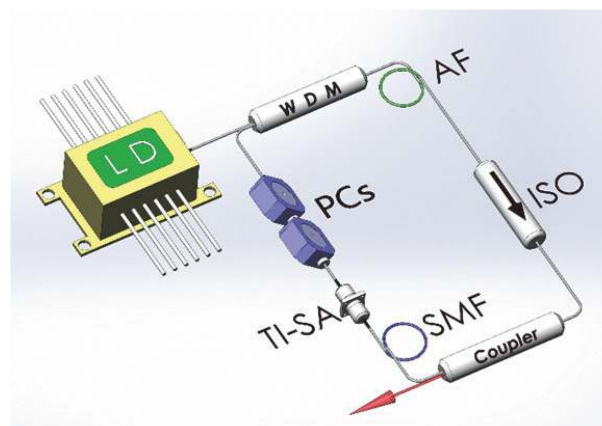

Figure 3: The schematic of mode-locked fiber laser.

3. Bi_2Te_3 Saturable Absorber Based Fiber Laser

3.1. Design of Mode-Locked Fiber Laser. To construct a passively mode-locked ring fiber laser, the experimental configuration as in Figure 3 is employed, including the standard fiber-optic components such as wavelength division multiplexer (WDM), polarization controller (PC), coupler, optical isolator, and active fiber (AF). The fiber laser has a ring cavity configuration with a total cavity length of 15.22 m, which comprises a piece of 1 m erbium-doped fiber (EDF, LIEKKI Er 80-8/125) as AF with group velocity dispersion (GVD) of -20 ps^2/km and the pigtails of fiber-optic components. All these pigtails are standard single mode fiber (SMF-28) with GVD of -23 ps^2/km at 1550 nm. The pump, which was generated from a 975 nm laser diode (LD) source, is coupled into the cavity through a 980/1550 wavelength-division multiplexer (WDM), and a 10% fiber coupler is employed to output the pulsed laser. A polarization independent isolator (PI-ISO) is used to force the unidirectional operation of the ring cavity, and a polarization controller (PC) is used to fine adjust the polarization state of circulating light and the in-cavity

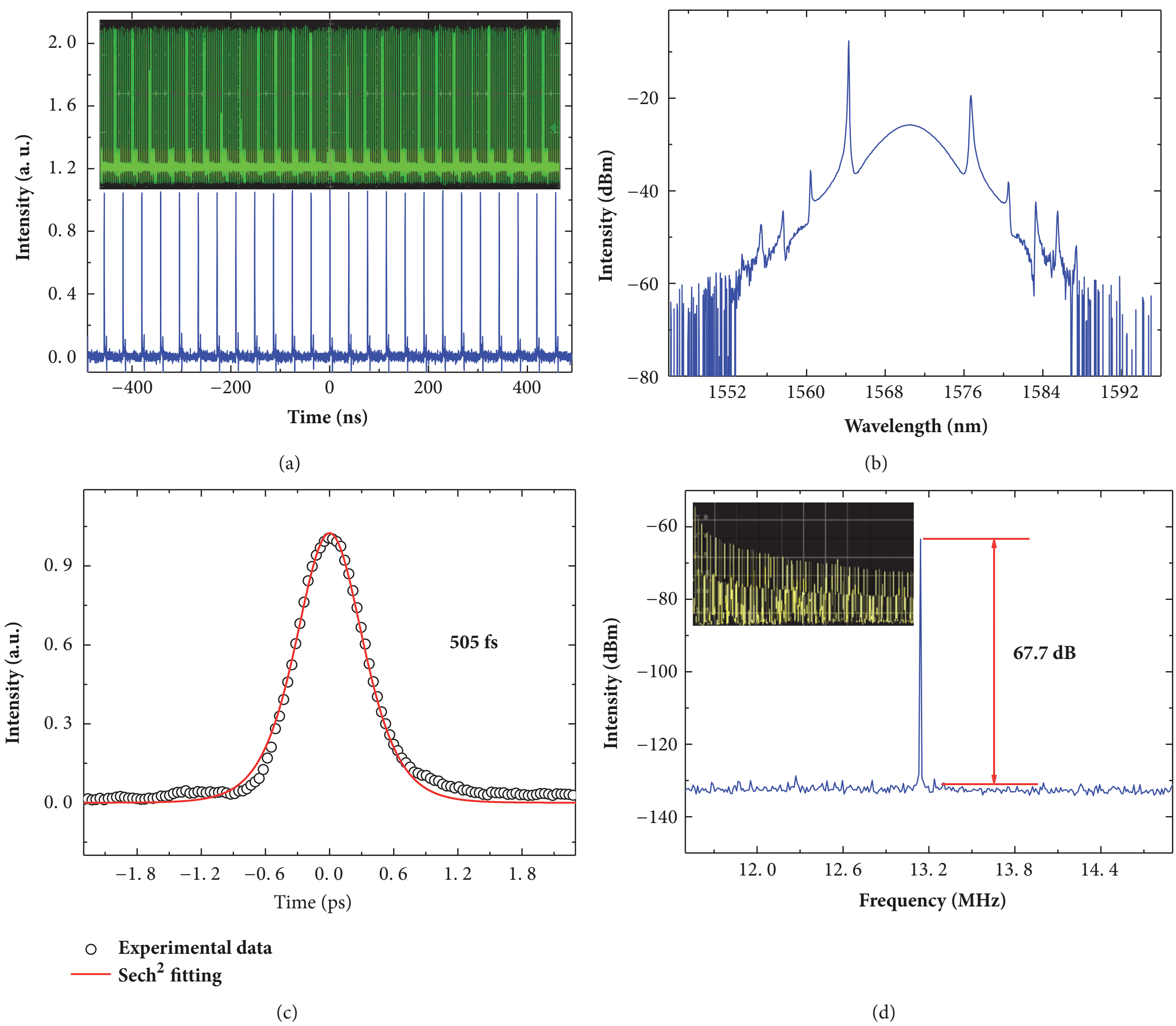

FIGURE 4: Single pulse mode-locking results of fiber laser.

birefringence. An optical spectrum analyzer (Ando AQ-6317B) and an oscilloscope (Tektronix TDS3054B) combined with a 5 GHz photo-detector (Thorlabs SIR5) are employed to simultaneously monitor the optical spectra and temporal profile of the output pulse. The pulse duration is measured with a commercial second harmonic generation autocorrelator.

3.2. Mode-Locking Results and Discussions. The mode-locking operation could be self-started with a mode-locking threshold of 63.7 mW. Figure 4 summarizes the characteristics of single soliton pulse of our fiber laser at pump power of 85.4 mW. Figure 4(a) shows that the single pulse train with a repetition rate of 13.14 MHz, which matches well with the cavity length, indicates that the laser operates in the mode-locking state. The corresponding optical spectrum, as shown in Figure 4(b), has obvious Kelly sidebands spectral indicating that the fiber laser operates in soliton regime. It has a central wavelength of 1570.45 nm and a 3 dB bandwidth of 5.35 nm. Correspondingly, as shown in Figure 4(d), the measured autocorrelation (AC) trace can be well fitted by hyperbolic secant function with a full width at half maximum (FWHM) of 756 fs, showing that the real pulse width is about 505 fs. The time-bandwidth product is 0.328, indicating that the obtained soliton pulse is almost transform limited. Figure 4(d) is corresponding measured RF spectrum with resolution bandwidth (RBW) of 10 Hz; the signal-to-noise ratio (SNR) of our fiber laser is up to 67.7 dB indicating that our fiber laser operates in a relatively stable regime. Moreover, as can be seen in long scale RF spectrum (the insert), there is not any excrescent frequency components except the fundamental and harmonic frequency components, further confirming the stability of our fiber laser and single soliton operation.

To investigate the long-term stability of the single soliton operation, we recorded the output spectra every hour over 6 h with fixed experimental setup, such as pump power of 90 mW, as shown in Figure 5. Neither the central wavelength drift

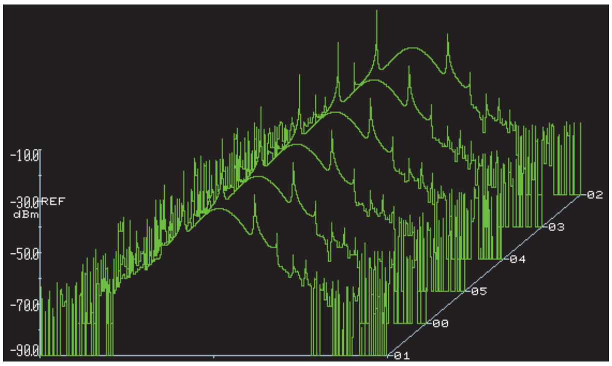

Figure 5: Long-term stability of optical spectra.

nor new wavelength component was observed during our measurement and always exhibits the same profiles, showing excellent repeatability and superimposability. All these results confirm the fiber laser possesses a reasonably good stability that is suitable for practical applications.

During the entire measurement, neither the central wavelength drifting nor new wavelength components were observed, revealing that the mode-locked fiber laser shows long-term stability, which benefits from the PMMA sandwiched Bi_2Te_3 nanosheets saturable absorber. There are many other advantages to this novel PMMA-TI-PMMA structure. First, the spin coated layer spontaneously generated at the interface between the solution and air can remain very uniform. Second, the spin coated layer can be effectively protected by double PMMA layers, and the original morphology will be automatically kept while being transferred and installed. Third, the saturable absorber device can be effectively protected from oxidation, since it is isolated from air and water due to the double PMMA sandwich structure. Also, this mode-locked result shows no distinct different with previous reports [28–30], which means that this transfer process has no adverse effect to the Bi_2Te_3 based saturable absorber. All of these results lead to a conclusion: the PMMA sandwiched structure could protect well the Bi_2Te_3 based saturable absorber and ensure no recede of the performance of saturable absorber.

4. Conclusions

Here, we fabricated a PMMA sandwiched Bi_2Te_3 nanosheets structure process. Based on this PMMA sandwiched Bi_2Te_3 nanosheets saturable absorber, we have demonstrated stable mode-locked fiber laser. Ultrafast pulse with a pulse width about 505 fs was obtained from the mode-locked fiber laser. These results suggest that the PMMA sandwiched Bi_2Te_3 nanosheets structure is a good saturable absorber candidate for ultrafast pulse generation. Also this technique could be developed to fabricate other stable two-dimensional materials based devices.

Data Availability

The experimental data used to support the findings of this study are all included within the article.

Conflicts of Interest

The authors declare that they have no conflicts of interest.

Acknowledgments

This work was partially supported by the Natural Science Foundation of Hunan Province, China (Grant no. 2018JJ2455).

References

[1] J. E. Moore and L. Balents, "Topological invariants of time-reversal-invariant band structures," *Physical Review B: Condensed Matter and Materials Physics*, vol. 75, no. 12, 2007.

[2] L. Fu, C. L. Kane, and E. J. Mele, "Topological insulators in three dimensions," *Physical Review Letters*, vol. 98, no. 10, 2007.

[3] L. Fu and C. L. Kane, "Topological insulators with inversion symmetry," *Physical Review B: Condensed Matter and Materials Physics*, vol. 76, no. 4, 2007.

[4] J. C. Y. Teo, L. Fu, and C. L. Kane, "Surface states and topological invariants in three-dimensional topological insulators: Application to Bi1-x Sbx," *Physical Review B: Condensed Matter and Materials Physics*, vol. 78, no. 4, 2008.

[5] D. Hsieh, D. Qian, L. Wray et al., "A topological Dirac insulator in a quantum spin Hall phase," *Nature*, vol. 452, no. 7190, pp. 970–974, 2008.

[6] H. Zhang, C.-X. Liu, X.-L. Qi, X. Dai, Z. Fang, and S.-C. Zhang, "Topological insulators in Bi_2 Se_3, Bi_2 Te_3 and Sb_2 Te_3 with a single Dirac cone on the surface," *Nature Physics*, vol. 5, no. 6, pp. 438–442, 2009.

[7] Y. L. Chen, J. G. Analytis, J.-H. Chu et al., "Experimental realization of a three-dimensional topological insulator, Bi_2Te_3," *Science*, vol. 325, no. 5937, pp. 178–181, 2009.

[8] C. Zhao, H. Zhang, X. Qi et al., "Ultra-short pulse generation by a topological insulator based saturable absorber," *Applied Physics Letters*, vol. 101, no. 21, 2012.

[9] C. Zhao, Y. Zou, Y. Chen et al., "Wavelength-tunable picosecond soliton fiber laser with Topological Insulator: Bi_2Se_3 as a mode locker," *Optics Express*, vol. 20, no. 25, pp. 27888–27895, 2012.

[10] U. Keller, "Recent developments in compact ultrafast lasers," *Nature*, vol. 424, no. 6950, pp. 831–838, 2003.

[11] G. Steinmeyer, D. H. Sutter, L. Gallmann, N. Matuschek, and U. Keller, "Frontiers in ultrashort pulse generation: Pushing the limits in linear and nonlinear optics," *Science*, vol. 286, no. 5444, pp. 1507–1512, 1999.

[12] F. Wang, A. G. Rozhin, V. Scardaci et al., "Wideband-tuneable, nanotube mode-locked, fiber laser," *Nature Nanotechnology*, vol. 3, pp. 738–742, 2008.

[13] F. Bonaccorso, Z. Sun, T. Hasan, and A. C. Ferrari, "Graphene photonics and optoelectronics," *Nature Photonics*, vol. 4, no. 9, pp. 611–622, 2010.

[14] S. Wang, H. Yu, H. Zhang et al., "Broadband few-layer MoS_2 saturable absorbers," *Advanced Materials*, vol. 26, no. 21, pp. 3538–3544, 2014.

[15] J. Du, Q. Wang, G. Jiang et al., "Ytterbium-doped fiber laser passively mode locked by few-layer Molybdenum Disulfide (MoS2) saturable absorber functioned with evanescent field interaction," *Scientific Reports*, vol. 4, no. 1, 2015.

[16] F. Xia, H. Wang, and Y. Jia, “Rediscovering black phosphorus as an anisotropic layered material for optoelectronics and electronics,” *Nature Communications*, vol. 5, p. 4458, 2014.

[17] Y. Chen, G. Jiang, S. Chen et al., “Mechanically exfoliated black phosphorus as a new saturable absorber for both Q-switching and mode-locking laser operation,” *Optics Express*, vol. 23, no. 10, pp. 12823–12833, 2015.

[18] C. Zhao, H. Zhang, X. Qi et al., “Ultra-short pulse generation by a topological insulator based saturable absorber,” *Applied Physics Letters*, vol. 101, Article ID 211106, 2012.

[19] Y. Chen, C. Zhao, S. Chen et al., “Large energy, wavelength widely tunable, topological insulator Q-switched erbium-doped fiber laser,” *IEEE Journal of Selected Topics in Quantum Electronics*, vol. 20, no. 5, pp. 315–322, 2014.

[20] S. Chen, C. Zhao, Y. Li et al., “Broadband optical and microwave nonlinear response in topological insulator,” *Optical Materials Express* , vol. 4, no. 4, pp. 587–596, 2014.

[21] G. Jiang, J. Yi, L. Miao et al., “Bismuth Telluride nanocrystal: broadband nonlinear response and its application in ultrafast photonics,” *Scientific Reports*, vol. 8, no. 1, 2018.

[22] S. Chen, Y. Chen, M. Wu, Y. Li, C. Zhao, and S. Wen, “Stable Q-Switched Erbium-Doped Fiber Laser Based on Topological Insulator Covered Microfber,” *IEEE Photonics Technology Letters*, vol. 26, pp. 987–990, 2014.

[23] M. Wu, Y. Chen, H. Zhang, and S. Wen, “Nanosecond Q-switched erbium-doped fiber laser with wide pulse-repetition-rate range based on topological insulator,” *IEEE Journal of Quantum Electronics*, vol. 50, no. 6, pp. 393–396, 2014.

[24] B. S.-Y. Ung, B. Weng, R. Shepherd, D. Abbott, and C. Fumeaux, “Inkjet printed conductive polymer-based beam-splitters for terahertz applications,” *Optical Materials Express* , vol. 3, no. 9, pp. 1242–1249, 2013.

[25] Y. Chen, C. Zhao, H. Huang et al., “Self-assembled topological insulator: Bi_2Se_3 membrane as a passive Q-switcher in an erbium-doped fiber laser,” *Journal of Lightwave Technology*, vol. 31, no. 17, pp. 2857–2863, 2013.

[26] H. Zhang, Q. Bao, D. Tang, L. Zhao, and K. Loh, “Large energy soliton erbium-doped fiber laser with a graphene-polymer composite mode locker,” *Applied Physics Letters*, vol. 95, no. 14, Article ID 141103, 2009.

[27] Q. Wang, Y. Chen, L. Miao et al., “Wide spectral and wavelength-tunable dissipative soliton fiber laser with topological insulator nano-sheets self-assembly films sandwiched by PMMA polymer,” *Optics Express*, vol. 23, no. 6, pp. 7681–7693, 2015.

[28] Q. Wang, Y. Chen, G. Jiang et al., “Drop-casted self-assembled topological insulator membrane as an effective saturable absorber for ultrafast laser photonics,” *IEEE Photonics Journal*, vol. 7, no. 2, 2015.

[29] J. Liu, M. Wu, B. Huang et al., “Widely Wavelength-Tunable Mid-Infrared Fluoride Fiber Lasers,” *IEEE Journal of Selected Topics in Quantum Electronics*, vol. 24, no. 3, pp. 1–7, 2018.

[30] B. Huang, P. Tang, J. Yi et al., “Resonantly pumped Er:YAG laser Q-switched by topological insulator nanosheets at 1617 nm,” *Optical Materials*, vol. 71, 2016.